Title

OPTIMIZATION OF Fe/Cr/C BASE STRUCTURAL STEELS FOR IMPROVED STRENGTH AND TOUGHNESS

Authors

Sarikaya, M.
Steinberg, B.G.
Thomas, G.

Publication Date

1981-05-01

LBL-11421
Preprint

Lawrence Berkeley Laboratory
UNIVERSITY OF CALIFORNIA

Materials & Molecular Research Division

Submitted to Metallurgical Transactions

OPTIMIZATION OF Fe/Cr/C BASE STRUCTURAL STEELS FOR IMPROVED STRENGTH AND TOUGHNESS

M. Sarikaya, B.G. Steinberg, and G. Thomas

May 1981

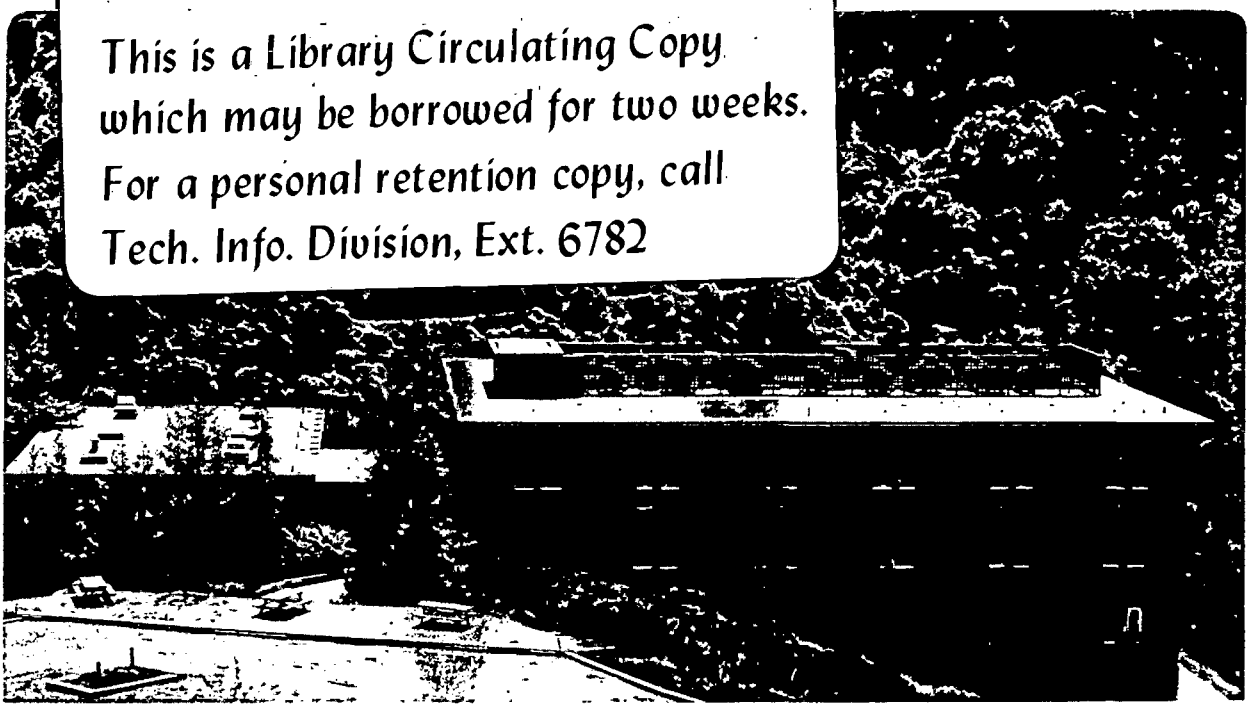

Prepared for the U.S. Department of Energy under Contract W-7405-ENG-48

DISCLAIMER

OPTIMIZATION OF Fe/Cr/C BASE STRUCTURAL STEELS FOR IMPROVED STRENGTH AND TOUGHNESS

M. Sarikaya, B. G. Steinberg and G. Thomas

Materials and Molecular Research Division

Lawrence Berkeley Laboratory

and

Department of Materials Science and Mineral Engineering

University of California

Berkeley, California 94720

This work was supported by the Director, Office of Energy Research, Office of Basic Energy Sciences, Materials Sciences Division of the U.S. Department of Energy under Contract No. W-7405-ENG-48. M. Sarikaya would like to thank the TUBITAK-BAYG for the NATO Science Scholarship.

ABSTRACT

Optimization of the composition and the heat treatments to provide microduplex structure of dislocated-autotempered lath martensite and thin film retained austenite for good combinations of mechanical properties has been attained for Fe/Cr/C base steels. Substituting 0.5 wt% Mo to reduce Cr from 4% to 3% did not affect the microstructures nor the properties. It was found that air melting does not cause deterioration of toughness in Mn containing alloys but does so in Ni containing alloys. Tempered martensite embrittlement was confirmed as being due to the decomposition of retained austenite. Further improvements in the fracture toughness are achieved by double heat treatments which attain grain refinement. These alloys are very promising for structural applications.

I. INTRODUCTION

It is well known that the martensitic transformations can be exploited to produce a wide variety of strength values by simply changing the alloy content, especially carbon, (e.g. refs. 1, 2). However, increases in strength are usually associated with corresponding decreases in the toughness values limiting the extent of structural applications of steels.[3] An approach to overcome this problem by microstructural control (duplex structures) involving ternary and quarternary additions of substitutional alloying elements,[4-7] and changes and/or variations in the heat treatments,[5-7] has, for example, led to the development of experimental Fe/4Cr/0.35C structural steels which have superior strength-toughness combinations over more complex commercial steels, and which are used as the base material for the present study (see ref. 7 for review).

In the as-quenched condition, the microstructure of the base steel consists of heavily dislocated autotempered lath martensite and thin films of retained austenite at the lath boundaries. In fact, large increases in toughness in these and commercial steels have been attributed[4,7,8] to the presence of stable, retained austenite which is found in these duplex structures. To improve the toughness to strength ratio, steels are usually tempered following quenching. Retained austenite becomes thermally unstable following 300-400°C tempering which is associated with loss in toughness and ductility (tempered martensite embrittlement).[10]

The objective of the current investigation is to further improve the properties of the base steel through careful microstructural control via modifications in the alloying additions and heat treatments, and

also to explore the properties from air melted alloys since previous data[4-7] were all obtained from vacuum melted alloys.

The Cr content was decreased from its original value of 4 wt%[4,7] to 3 wt% and 0.5 wt% Mo was added to compensate for the loss in hardenability.[9] Having the effect of temper resistance[3] in retained austenite, Mo may limit and postpone the onset of tempered martensite embrittlement (TME),[10] although in Fe/Mo/C steels, little or no austenite was detected.[11] C is necessary to increase strength and it is vital to obtain retained austenite. Mn and Ni additions were made mainly to stabilize the retained austenite in the presence of C.[7,10] The level of the alloying additions followed previous considerations.[7]

Higher austenitizing temperatures than 900°C can be beneficial to the mechanical properties of HSLA steels.[5,7,8] By high temperature (>1100°C) treatment, coarse alloy carbides can be dissolved completely and a compositionally homogeneous structure can be achieved.[7,8] However, a very high austenitizing temperature leads to an increase in grain size. Yield strength and fracture toughness (CVN) values increase and DBTT decreases with a decrease in prior austenite grain size.[12] This also decreases the severity of embrittling constituents.[13] Once a compositionally homogeneous structure is achieved by heat treatments, grain refinement increases the amount of retained austenite.[7] Therefore, double austenitizing, i.e., high-temperature austenitizing and quenching followed by low-temperature austenitizing, can be applied to obtain the benefits of both treatments. In each case the aim was to produce the duplex microstructure sketched in fig. 1.

II. EXPERIMENTAL PROCEDURE

The alloys used in this investigation were either vacuum induction melted or air melted in 20 lb. ingots and subsequently rolled to

1 in. thick, 2.5 in. wide, and 25 in. long slabs. All the alloys were sand blasted to remove any oxide scale and homogenized at 1200°C for 24 hours in vacuo before furnace cooling. The compositions of the alloys (Table I) were measured after this process. The C content was also measured after subsequent heat treatments to check for any decarburization.

Plain strain fracture toughness and Charpy V-notch impact toughness specimens were obtained from these slabs. Round tensile specimens were obtained from 0.75 in. diameter rods. The M_s, M_f (95%), A_s, A_f were determined by dilatometric measurements (Table I).

Basically, three kinds of heat treatments were applied as shown schematically in Fig. 2. They involve high and/or low temperature austenitizing, quenching in oil, and subsequent tempering. All the austenitizing treatments were carried out in a vertical tube furnace under dynamic argon atmosphere. Oversized tensile, Charpy, and K_{IC} specimens were cut from the homogenized material and machined to blanks. After austenitizing 1 hr. they were quenched in agitated oil. Tempering treatments (200°C-600°C) were given in a salt pot and then the specimens were quickly quenched into water. Final machining was done under flood cooling to avoid any heating.

All mechanical tests and specimens, Charpy V-notch, tensile and plain strain fracture toughness (K_{IC}), were designed to ASTM standards.[12] The 1.25 in. gauge round tensile specimens were pulled on a 300 Kip (1.33 MN) MTS testing machine at crosshead speed of 0.04 in/min. at room temperature. The K_{IC} specimens were pre-fatigue cracked and subsequently pulled in the same machine to obtain the plane strain fracture toughness values. Charpy impact testing was conducted with a 224-ft-lb

capacity impact device. All mechanical testings were performed at room temperature except for obtaining the ductile-to-brittle transition temperature (DBTT).

Microstructural determination was conducted on the optical and transmission electron microscopy (TEM) levels. Specimens for optical metallography were prepared by using standard techniques and etched in 2% nital. An AMR-1000 scanning electron microscope operated at 20kV was utilized to conduct fractographic studies and energy dispersive x-ray analysis was used to analyze the inclusions semiquantitatively.

Thin foils for TEM were obtained from broken Charpy specimens. About 0.020 in. (500μm) slices were cut longitudinally with a 1/32 in. (800μm) thick abrasive wheel under flood cooling. 3 mm discs were spark cut from these slices which were already chemically thinned to about 0.004 in (∿100 m) in 5% Hf-H_2O_2 solution. Discs were carefully sanded down to about 0.002 in. (50μm) and then electropolished in a twin-jet electropolishing apparatus at room temperature using CHROMACEDIC solution (75gm CrO_3 + 400ml CH_3-COOH + 20ml H_2O) at a voltage range of 40-45 volts, and 50-55 milliamperes. Subsequently, foils were examined by either JEM-7A or Philips EM-301 electron microscopes operated at 100kV.

III. RESULTS

Microstructural Characterizations

(i) Optical Metallography. Optical metallography showed that there were no major differences in the apparent microstructures of the alloys under different heat treatment conditions. The structures are composed of martensite packets containing laths. There were no undissolved carbides detected in the structures. Generally, the microstructures of the air melted alloys (i.e. 1A and 2A) are very similar

to vacuum melted ones (i.e. 1V and 2V, see Table I). However, as can be seen in Fig. 3, some undissolved inclusions are noticeable in both of the air melted alloys.

For heat treatment II, the average grain size decreases significantly in alloys V1 and V2, but the size is not uniform. However, following the application of H.T.(III), a decrease in size and uniformity of grains was noticeable, see Table II.

(ii) Transmission Electron Microscopy. Detailed characterization of microstructures at all levels of heat treatment was performed on all the alloys studied. Here the results obtained in the alloys V1 and V2 are included, since the air melted alloys of similar compositions showed similar microstructural variations.

(a) Structure of the Alloys in the As-Quenched Condition. The morphology of martensite in these alloys is lath type.[1,2,15-17] In certain packets the laths of average width about 0.5μm, are fairly straight and parallel to each other (Fig. 4). Two very important substructural variations were observed in these alloys, i.e., microstructural twinning and autotempered carbides. Although most parts of all martensite laths are heavily dislocated, a small amount of $\{112\}_\alpha$ substructural twinning has also been observed in both steels. However, the amount of microtwinning in the 2% Ni containing steel, alloy V2, was much lower than that of the 5 wt% Ni containing base steel[7] and higher than the Mn containing steel, alloy V1. Significant amounts of autotempering in both alloys are attributed to high M_s temperatures (Table I). $\{110\}_\alpha$ Widmanstätten cementite was observed in the alloy V1, while ε-carbides were predominant in the alloy V2.

(b) Structure of the Alloys in the Tempered Conditions. Upon 200°C tempering, $\{110\}_\alpha$ Widmanstätten cementites were observed in both alloys. However, ε-carbides were still present in alloy V2 (Figs. 5c and d). The amount of interlath carbide precipitation greatly increased following 300°C tempering. While new carbides start forming, existing ones coarsened. At this tempering temperature ε-carbides in Ni-containing steel were replaced by cementite (Fig. 6). The size of cementite precipitates at this tempering was about 0.1-0.2μm long and 50-100Å wide. No spheroidization of carbides was observed at this condition. However, carbides started to form on microstructural twins (Fig. 6). By 400°C tempering carbides continue to grow and start spheroidizing. At higher tempering temperatures (500 and 600°C), spheroidization is more advanced. Carbides precipitated within laths and on microstructural twins grow further. No alloy carbides would be identified even upon this temperature tempering.

(c) Retained Austenite. Although the bulk M_s and M_f temperatures of the steels were well above room temperature, viz., $M_s > 300°C$, significant amounts (~4% by volume) of retained austenite were found at the lath boundaries. This phase in the as-quenched and 200°C tempered condition is in the form of a very thin (150-200Å) and continuous film between the martensite laths (Fig. 7). By tempering the steel at higher temperatures, the stability of retained austenite changed. Following 300°C tempering, there was no retained austenite present in the Mn-alloy. Instead, as a result of decomposition of retained austenite, coarse carbides precipitated at the lath boundaries (Fig. 8). This

decomposition reaction occurred after 400°C tempering in Ni-containing steel, which resulted in discontinuous coarse stringers of carbides which are identified as cementite. This microstructure is analogous to that of upper bainite.[10]

(d) Structure of the Modified Heat Treated Steels. By the application of a grain refining heat treatment, i.e., H.T. (II), Fig. 2, essentially the same type of morphologies as those seen following single heat treatment were observed. Structures were examined after 200°C tempering. Only cementite precipitation occurred in alloy V1, while ε-carbide precipitation was dominant in alloy V2. Martensite lath boundaries were decorated by narrow films of retained austenite. The application of H.T. (III) resulted in the same type of substructural features but the overall amount of retained austenite seemed to be higher.

Mechanical Properties

The mechanical properties of both steels are tabulated in Tables III, IV, and V. In order to see the trend of the mechanical behavior with respect to heat treatment, the values are plotted as a function of tempering temperature, Figs. 9-10. In the as-quenched condition, yield strength values of the alloys in both melting conditions are about 200 ksi, the same as in the base steel.[7] Somewhat higher strength values for alloys A1 and A2 may be attributed to a slighly higher C content in these steels. Fracture properties are qualified via both plane strain fracture toughness (K_{IC}) and Charpy V-notch impact toughness tests. The somewhat low K_{IC} values for all cases in the as-quenched condition were improved greatly by tempering at 200°C concommitant

with a slight increase in yield strength, Fig. 11. In fact, this is the condition for the best properties for the single treated steels.

The most dramatic variations occur in the CVN-Impact values with increasing tempering temperature, Fig. 10. Following 200°C tempering, impact values increase significantly as compared to the values in the as-quenched condition. The fractographic study showed ductile dimpled rupture (transgranular) in all the alloys. A very sharp decrease occurs in the Mn containing steels after 300°C tempering (Fig. 10). Changes in the fracture mode, i.e., brittle quasi cleavage fracture (transgranular with respect to prior austenite grain boundaries, but intergranular with respect to martensite lath boundaries) with parallel ridges of the order of lath widths on the surface of the alloys V1 and V2, are evident (Fig. 12a). Although the impact value is not that severely affected in alloy V2 (Fig. 10), almost the same type of fracture surface appearance can be seen following 400°C tempering (Fig. 12b). A second minimum occurs for the Mn-steels following 500°C tempering which was associated with complete intergranular fracture. However, the behavior was quite different for A2 which showed rather low CVN-energy and K_{IC} values both in the as-quenched and 200°C tempered condition, i.e., the condition of highest interest. Surprisingly enough, alloy A2 exhibited a higher density of particles (mostly oxide inclusions) than alloy A1 (Mn-containing alloy), and long "striations" or rib-like features in all tempering ranges (e.g. see Fig. 13). These features average approximately 15-20μm in length with the internal ribs fairly evenly spaced at 1-1.5μm.

By the application of single high temperature austenitization, i.e., H.T.(I), steels show significantly high CVN-Impact energy values compared to conventional low temperature austenitization, i.e. H.T.(C) (Fig. 11). In addition, double heat treatments were applied to vacuum melted alloys, since they are structurally homogeneous. Generally, trends of improvements in both K_{IC} and CVN-Impact energy values were achieved with no significant change in strength values (Fig. 11). Following 200°C tempering after austenitizing treatment(s), significant improvements almost always occur in the fracture values, while slight increases in yield strength values are also apparent (Fig. 11).

Ductile to brittle transition temperatures in the vacuum melted steels are much lower and narrower than the air melted steels (Fig. 14). Compared to others, the range is much narrower for alloy V1, i.e., -150 to 50°C, and the impact energy has an upper shelf of about 30 ft-lb.

IV. SUMMARY AND DISCUSSION

1. Variations in Microstructures

The morphology of martensite in all the steels was basically dislocated lath martensite[1,2,15,17,18] (Fig. 4). However, sometimes substructural twinning was observed (Fig. 6) which mainly affects the toughness of the steels,[4,7] especially in the tempered condition where carbides preferentially precipitate on twins (Fig. 6) which can then act as easy crack paths. The existence of the desired interlath austenite at room temperature in these steels has been attributed to several mechanisms,[7] one of the most important being high carbon contents, as revealed by high resolution lattice imaging[19] and field ion atom probe studies.[20]

Due to the high M_s temperatures ($\sim$ 300°C), an extensive amount of auto-tempering occurred in the steels (Fig. 4). During quenching, after the formation of martensite, C atoms have enough time to redistribute themselves around dislocations and cell walls.[20] These clusters then grow to form carbides following low temperature tempering (Fig. 5). Microstructural changes during tempering follow as discussed in Results.

2. Summary of Mechanical Properties and Microstructural Changes

By the application of high temperature austenitization, i.e. 1100°C, coarse alloy carbides were dissolved in the steels and a compositionally homogeneous austenite phase was obtained. Even in the as-quenched condition, mechanical properties are very good (Tables III-IV, Figs. 9-11). Somewhat lower strength values in the vacuum melted steels may be attributed to the slightly lower (0.22 wt%) C content in the tensile bars. A small increase in the yield strength (Fig. 9) and significant improvements in CVN-Impact energy and K_{IC} values (Fig. 11) upon 200°C tempering may be due to newly formed, very small carbides which increase the flow stress in martensite (Fig. 5). High toughness values in the as-quenched and 200°C tempered conditions may also be attributed to mechanically more stable austenite films at the lath boundaries (Fig. 7). In the temperature range 300-500°C, a levelling-off behavior in the tensile strength vs. tempering temperature graphs due to temper resistance in all of the alloys is observed (Fig. 9). Before this temperature regime, ε-carbide to cementite transformation takes place. Interesting events occur in the structure in the 300-500°C temperature range due to different types of embrittlements.

Both "Tempered Martensite Embrittlement" (TME)[7,10,21,22] and "Temper Embrittlement" (TE)[7,13] were observed. These phenomena and observed temperatures may be explained in conjunction with the behavior of retained austenite, carbide formation, and segregation of residual elements. Retained austenite was stable following 200°C tempering in both alloys. But following 300°C tempering, austenite decomposes in the Mn containing alloy (Fig. 8). The same type of transformation occurs following 400°C tempering in Ni-containing steel. Since the decomposition reaction occurs well above M_s temperature (due probably to the solute, especially C, enrichment in retained γ), it has been speculated to be upper bainitic.[7,16] Formation of stringers of coarse carbides at the lath boundaries provide easy crack paths (Fig. 12). The formation and growth of cementite are important in cementite precipitation from austenite. Mo limits the formation and growth of cementite in steel. But apparently this influence of Mo was not effective in the Mn containing steel, perhaps due to the small Mo content, viz., 0.5 wt%. However, the fact that TME, also known as "500°F embrittlement" occurs at higher tempering temperatures in Ni-containing steel may be a result of Ni being a graphitizing element. Hence, in the presence of Ni concurrent with Mo, higher temperatures are necessary to transform retained austenite to carbides. At higher temperature tempering, viz., 500°C, a second embrittlement, called TE, occurred in Mn-containing steel. The difference is that the fracture path is inter-martensite lath in TME and along prior austenite grain boundaries, i.e. trans- and intergranular with respect to prior austenite, respectively. This is generally believed to be caused by the segregation of impurities to

the prior austenite grain boundaries, which then lose cohesion [13,19] causing intergranular fracture. TE, together with TME, decreases toughness values even further in Mn-containing steel (Fig. 10). However, the fact remains that the presence of Mo in the steel seems to decrease the synergistic effects of TME and TE by increasing the Charpy values to higher levels (compare with Fig. 13a of Ref. 7). There was no significant change in the failure mode upon high temperature tempering of the Ni-containing steel. Therefore, TE does not occur in alloys V2 and A2. Following higher temperature tempering (i.e. > 500°C), whilst the strength values continue to decrease (Fig. 15), the impact toughness values increase probably due to the recovery of the martensitic substructure.

When the alloy containing manganese, A1, is air melted, little or no change is seen in the mechanical properties with respect to vacuum melted alloys, while the alloy containing nickel, A2, experiences a marked drop in toughness and ductility (Table IV and Fig. 10). Fracture surfaces reveal that there is a considerable increase in the amount of second-phase particles within the 2Ni steel. Ductility decreases with secondary particle volume percent as void formation, growth, and coalescence begins around particles.[23] Another feature seen in the SEM fractographs is the existence of rib-like fractures in all tempering ranges of the nickel steel (Fig. 13). This type of fracture is too large to be at interlath boundaries and does not follow any set direction. It is thus likely to be caused by linear coalescence of voids, which may be an end result of linear conglomeration of oxides, leading to premature fracture.

Upon application of H.T.(II), improvements in the fracture and impact properties were achieved (Fig. 11), while the strength values are slightly lower due to the increased amount of retained austenite. The overall effect of uniform and small grains of prior austenite and dissolution of carbides following H.T.(III) is reflected as a further increase in toughness values (Fig. 11). By the application of conventional heat treatment, viz., H.T. (C) (Fig. 2), steels showed brittle behavior (Fig. 11) probably because of a much lower amount of retained austenite and the presence of larger alloy carbides.

By the rearrangements of the alloying elements and the application of unconventional heat treatments, the desired microstructure (Fig. 1) was obtained. As a result of overall optimization, the experimental alloys, even air melted ones, especially A1, have superior strength and toughness combinations compared to the equivalent commercially used alloys as shown in Fig. 15.

V. CONCLUSIONS

Established alloy design guidelines[7] were followed for obtaining good strength and toughness combinations in optimizing Fe/Cr/C base low alloy steels for structural applications. Excellent properties were obtained, and these are correlated with the microstructural changes at each step of the heat treatments. The main conclusions achieved from this investigation are as follows:

(i) Decreasing the Cr content from 4wt% to 3wt% and adding 0.5wt% Mo to the base steel does not change the microstructural features and mechanical properties significantly.

(ii) This small addition of Mo was not enough to postpone TME to higher temperatures, but its presence increased the hardenability and decreased the severity of TE.

(iii) In alloy V2, decreasing Ni content from its original value of 5wt% to its present value of 2wt% caused a significant decrease in the amount of microtwinning, which was reflected in the increase of toughness properties. But a slight decrease in the amount of retained austenite was also evident.

(iv) Air melting did not greatly affect the microstructures and mechanical properties of Mn steels. Besides this, the 2wt% Mn containing steel, i.e. A1, has comparable strength-toughness combinations to its vacuum melted equivalent, i.e. V1. Hence, this alloy is a good candidate as an economical HSLA steel for structural applications.

(v) Air melted 2Ni alloy, i.e. A2, showed inferior toughness properties which were attributed to a high density of large second phase oxide particles, which caused linear coalescence of voids.

(vi) The fact that the Mn-containing alloys are very sensitive to the decomposition of retained austenite on tempering was reaffirmed. This phenomenon is the reason for the loss in toughness and ductility of these steels tempered in a 300-400°C regime.

(vii) It was shown that improvements in the toughness values, with little or no change in strength values, may be achieved by double heat treatments, high (1100°C) and low (900°C) temperature austenitizing with or without intermediate tempering. This combines the benefits of

attaining a homogeneous austenite phase free from alloy carbides and uniform/small austenite grains.

ACKNOWLEDGEMENTS

This work was supported by the Director, Office of Energy Research, Office of Basic Energy Sciences, Materials Science Division of the U. S. Department of Energy under Contract No. W-7405-ENG-48. One of the authors, M. Sarikaya, would like to thank the TUBITAK-BAYG for the NATO Science Scholarship. The authors are grateful to Dr. B. V. Narasimha Rao for many valuable discussions.

REFERENCES

1. G. Thomas: Iron, Steel, Int., 1973, vol. 46, pp. 451.
2. C. M. Wayman: Metallography, 1975, vol. 8, pp. 105.
3. R. W. K. Honeycombe: Structure and Strength of Alloy Steels, Climax Molybdenum Company, London, 1975.
4. J. McMahon and G. Thomas: Proc. Third International Conference on Strength of Metals and Alloys, vol. 1, pp. 180, Inst. of Metals, London, 1973.
5. B. V. Narasimha Rao, R. W. Miller and G. Thomas: Proc. 16th International Heat Treatment Conference, pp. 75, The Metals Society, London, 1976.
6. G. Thomas: Batelle Colloquium on Fundamental Aspects of Structural Alloy Design, R. I. Jaffee and B. A. Wilcox, eds., Plenum Publishing, 1977.
7. B. V. N. Rao and G. Thomas: Met. Trans., 1980, vol. 11A, pp. 441.
8. G. Y. Lai, W. E. Wood, R. A. Clark, V. F. Zackay and E. R. Parker: Met. Trans., 1974, vol. 5A, pp. 1663.
9. R. V. Fostini and F. J. Shoen: Symposium on Transformation and Hardenability in Steels, pp. 195, Climax Molybdenum Company, Ann Arbor, 1967.
10. G. Thomas: Met. Trans., 1978, vol. 9A, pp. 439.
11. R. A. Clark and G. Thomas; Met. Trans. A, Vol. 6A, pp. 969.
12. M. Carlson, B. V. N. Rao, R. O. Ritchie and G. Thomas: Proc. Intl. Conf. on Strength of Metals and Alloys 5, pp. 509, Nancy, France, 1976.

13. J. R. Rellick and C. J. McMahon, Jr.: Met. Trans., 1974, vol. 5, pp. 1151.

14. Standard Methods of Test for Plain Strain Fracture Toughness of Metallic Materials, Designation E399-7, Annual ASTM Standards, 1973, pp. 960.

15. P. M. Kelly and J. Nutting: JISI, 1961, vol. 183, pp. 199.

16. G. R. Speich and W. C. Leslie: Met. Trans. 1972, vol. 3, pp. 1043.

17. R. F. Hehemann, K. R. Kinsman, and H. I. Aaronson: Met. Trans., 1972, vol. 3, pp. 1077.

18. K. J. Irvine, F. P. Pickering, and J. Garstone: JISI, 1960, vol. 196, pp. 65.

19. B. V. Narasimha Rao and G. Thomas: Proc. of ICOMAT 1979, Boston, MIT Press, pp. 12-21.

20. S. Barnard, G. D. W. Smith, M. Sarikaya and G. Thomas: to be published in Scripta Met., 1981.

21. R. O. Ritchie and R. M. Horn: Met. Trans., 1978, vol. 9A, pp. 331.

22. H. K. D. H. Bhadeshia and D. V. Edmonds: Metal Science, June 1979, pp. 325.

23. T. B. Cox and J. R. Low, Jr.: Met. Trans., 1974, vol. 5A, pp. 1457.

TABLE I

ALLOY COMPOSITIONS AND TRANSFORMATION TEMPERATURES

Alloy	Composition, wt. pct.											Temperature, °C			
	Cr	C*	Mn	Ni	Mo	Si	Cu	Al	P	S	Fe	M_s	M_f	A_s	A_f
V1	3.11	0.26	1.98	0.01	0.50	0.07	0.01	-	0.007	0.011	Bal.	320	260	765	800
V2	3.01	0.25	0.08	2.00	0.51	0.07	0.01	-	0.007	0.009	Bal.	340	260	780	820
A1	2.94	0.29	1.86	0.03	0.52	0.01	0.02	0.04	0.017	0.009	Bal.	330	220	750	780
A2	3.19	0.30	0.10	2.11	0.48	0.15	0.01	0.05	0.007	0.012	Bal.	320	195	750	780

*In V1 and V2, wt. pct. of C is 0.22 and 0.24, respectively in the bars from which tensile specimens were prepared.

TABLE II

VARIATION OF PREAUSTENITE GRAIN SIZE

WITH HEAT TREATMENT PRACTICE

Alloy	Heat Treatment				
	I	II	III	C	
1V	270	40	35	30	Grain Size μm
2V	180	25	20	25	
1A	320	--	--	--	
2A	250	--	--	--	

TABLE III. VACUUM MELTED MECHANICAL PROPERTIES OF SINGLE TREATED STEELS*

Alloys**	H.T.(I) Tempering Temperature (°C)	Hardness (Rc)	0.2% Offset YS ksi	0.2% Offset YS MPa	UTS ksi	UTS MPa	% Elongation Total (Uniform)	K_{IC} ksi-in$^{1/2}$	K_{IC} MPa-m$^{1/2}$	Charpy V-notch Energy ft-lb	Charpy V-notch Energy N-m
	AQ	49	200	1378	253	1743	6.3(3.5)	80.0	89.0	28.7	39.0
	200	48	205	1413	257	1771	7.1(2.6)	110.5	123.0	34.5	46.8
V1	300	45	177	1220	206	1419	8.0(2.8)	-	-	22.5	30.5
	400	42	170	1171	200	1378	8.1(2.7)	-	-	22.0	30.0
	500	41	166	1144	194	1337	7.0(3.7	-	-	20.0	27.0
	600	35	126	868	144	992	14.6(4.5)	-	-	50.3	68.0
	AQ	50	197	1357	255	1757	8.1(3.3)	77.7	86.0	31.4	42.5
	200	48	199	1368	248	1709	8.9(3.2)	100.0	111.0	35.3	48.0
V2	300	44	173	1192	206	1419	9.4(2.4)	-	-	28.5	39.0
	400	43	167	1151	194	1337	10.5(2.6)	-	-	27.0	36.5
	500	40	160	1102	187	1288	12.2(3.1)	-	-	35.5	48.0
	600	36	129	885	146	1002	16.8(5.2)	-	-	90.3	122.5

*See Fig. 2

**See Table I

TABLE IV. MECHANICAL PROPERTIES OF AIR MELTED SINGLE TREATED* STEELS

Alloys**	Tempering Temperature °C	0.2% Offset YS_2 ksi	0.2% Offset YS_2 MPa	UTS ksi	UTS MPa	% Reduction in Area	% Elongation Total (Uniform)	K_{IC} ksi-in$^{1/2}$	K_{IC} MPa-m$^{1/2}$	Charpy V-notch Energy ft-lb	Charpy V-notch Energy N-m
A1	AQ	190	1306	263	1812	14.1	6.4(3.9)	104	115	29.8	40.3
	200	196	1353	238	1640	26.5	7.4(4.3)	117	130	39.9	54.2
	300	184	1266	223	1530	25.6	6.2(2.9)	-	-	14.9	20.3
	400	181	1249	213	1469	16.3	6.7(3.3)	-	-	13.3	18.1
	500	168	1159	201	1378	27.0	9.0(4.2)	-	-	10.6	14.3
	600	135	930	154	1060	46.2	12.8(4.4)	-	-	14.0	19.0
A2	AQ	207	1423	270	1863	16.7	7.2(4.0)	69	77	13.8	18.6
	200	202	1394	251	1727	19.0	13.7(3.9)	85	94	22.5	30.5
	300	186	1282	226	1554	19.0	9.6(3.0)	-	-	21.8	30.0
	400	181	1240	215	1481	15.4	10.5(3.5)	-	-	21.3	28.8
	500	171	1179	205	1413	30.1	14.2(4.2)	-	-	23.9	32.4
	600	140	965	160	1105	43.8	18.7(4.3)	-	-	47.8	64.8

*See Fig. 2

**See Table I

TABLE V. MECHANICAL PROPERTIES OF SINGLE AND DOUBLE TREATED STEELS

Heat Treatment**	Alloy*	Tempering Temperature	Hardness	YS ksi	YS MPa	UTS ksi	UTS MPa	% Elongation Total(Uniform)	K_{IC} ksi-in$^{1/2}$	K_{IC} MPa-m$^{1/2}$	Charpy V-notch Energy ft-lb	Charpy V-notch Energy N-m
		AQ	49	200	1378	253	1743	6.3(3.5)	80.0	89.0	28.7	39.0
	V1	200	48	205	1413	257	1771	7.0(3.6)	110.5	123.0	34.5	47.0
HT(I)		AQ	50	197	1357	255	1757	8.1(3.3)	77.7	86.0	31.4	42.5
	V2	200	48	199	1368	248	1709	8.9(3.2)	100.0	111.0	35.3	48.0
		AQ	49	194	1337	252	1736	9.6(3.5)	-	-	32.0	43.0
	V1	200	48	192	1319	250	1723	11.6(4.5)	116.0	128.5	38.0	51.5
HT(II)		AQ	49	196	1347	253	1742	10.1(3.5)	-	-	33.5	45.5
	V2	200	48	188	1295	245	1788	11.6(4.3)	93.5	104.0	38.0	51.5
		AQ	47	201	1385	259	1785	8.9(3.0)	-	-	35.0	48.0
	V1	200	47	194	1337	250	1723	12.0(4.5)	118.0	131.0	42.0	57.0
HT(III)		AQ	47	199	1371	252	1733	11.6(3.3)	-	-	43.0	46.5
	V2	200	47	195	1344	250	1723	11.8(4.5)	94.5	105.0	40.0	54.2
		AQ	45	199	1371	259	1785	8.9(4.0)	-	-	22.0	30.0
	V1	200	44	-	-	-	-	-	-	-	-	-
HT(C)		AQ	46	192	1323	248	1709	10.5(3.9)	-	-	22.5	27.0
	V2	200	44	-	-	-	-	-	-	-	-	-

*See Table I

**See Fig. 2

FIGURE CAPTIONS

Fig. 1. Schematic showing the desired microduplex structure consisting of dislocated lath martensite and thin films of retained austenite.

Fig. 2. Schematic illustration of heat-treatments employed.

Fig. 3. Optical micrographs of as-quenched steels: (a) A1 and (b) A2, showing the distribution of inclusions.

Fig. 4. A BF micrograph showing characteristic configuration of laths and packets in alloy V1 in the as-quenched condition. Notice three impringing packets, A, B, C.

Fig. 5. High magnification BF-DF micrographs show the carbide precipitation at 200°C tempered condition (H.T. (I)). (a) and (b) reveal Widmanstätten cementite in Mn containing alloy, i.e., V1; (c) and (d) ε-carbide in Ni containing alloy, i.e. V2.

Fig. 6. (a) BF and (b) DF of 300°C tempered alloy V2 revealing extensive carbide precipitation on the microstructural twins, on{121} . Also note the presence of Widmanstätten carbides in BF, (a).

Fig. 7. (a) BF, (c) DF micrographs and (b) indexed diffraction pattern from 200°C tempered alloy V2. Extensive amount of retained austenite in the form of films can be seen in the DF micrograph, (c).

Fig. 8. BF (a) and DF (b) showing the decomposition of retained austenite into interlath cementite stringers (indicated by arrows) in a 300°C tempered Mn containing alloy, V1.

Fig. 9. Strength vs. tempering temperature curves for Heat Treatment (I).

Fig. 10. A comparison of CVN-Impact energy vs. tempering temperature curves (H.T.(I)) for vacuum and air melted alloys (refer to Table I).

Fig. 11. Change in mechanical properties with heat treatment practice.

Fig. 12. (a) 300°C tempered alloy V1, and (b) 400°C tempered alloy V2 revealing parallel ridge appearance on the fracture surfaces after the decomposition of retained austenite.

Fig. 13. Fractograph showing the rib-like features (shown by arrows) which were probably caused by linear coalescence of voids in A2 (300° tempered condition).

Fig. 14. Ductile to Brittle Transition Temperatures (DBTT) for the alloys.

Fig. 15. The comparison of toughness to strength relations in the experimental alloy and equivalent commercial alloys. (a) CVN-Impact Energy vs. tensile strength, and (b) plain strain fracture toughness (K_{IC}) vs. tensile strength.

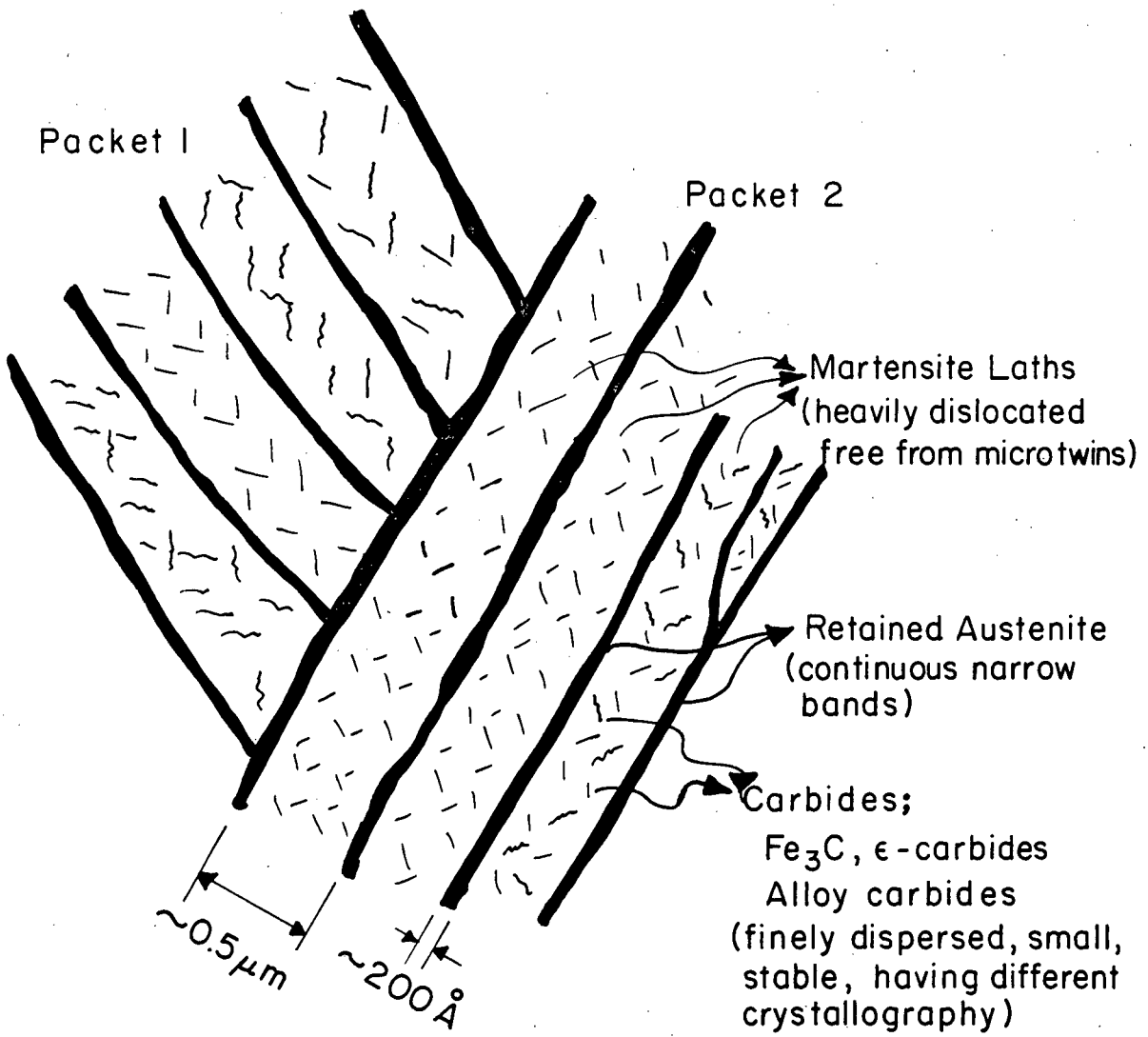
Packet 1
Packet 2
Martensite Laths
(heavily dislocated
free from microtwins)
Retained Austenite
(continuous narrow
bands)
Carbides;
Fe_3C, ε-carbides
Alloy carbides
(finely dispersed, small,
stable, having different
crystallography)
~0.5μm
~200Å
XBL794-6146

Fig. 1

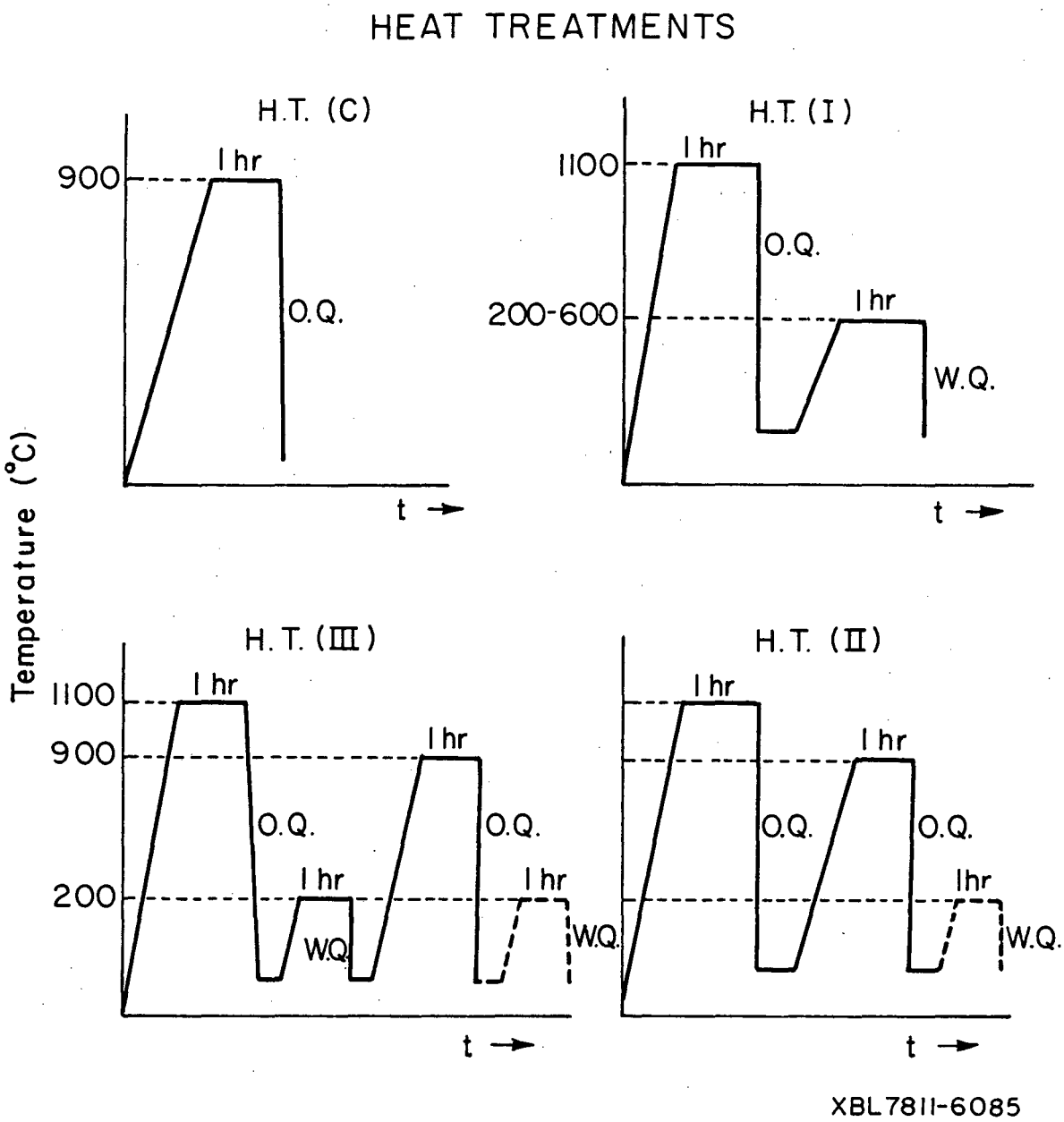
HEAT TREATMENTS
H.T. (C)
900
1 hr
O.Q.
t →
H.T. (I)
1100
1 hr
O.Q.
200-600
1 hr
W.Q.
t →
Temperature (°C)
H.T. (III)
1100
1 hr
900
1 hr
O.Q.
O.Q.
200
1 hr
1 hr
W.Q.
W.Q.
t →
H.T. (II)
1 hr
1 hr
O.Q.
O.Q.
1 hr
W.Q.
t →
XBL7811-6085

Fig. 2

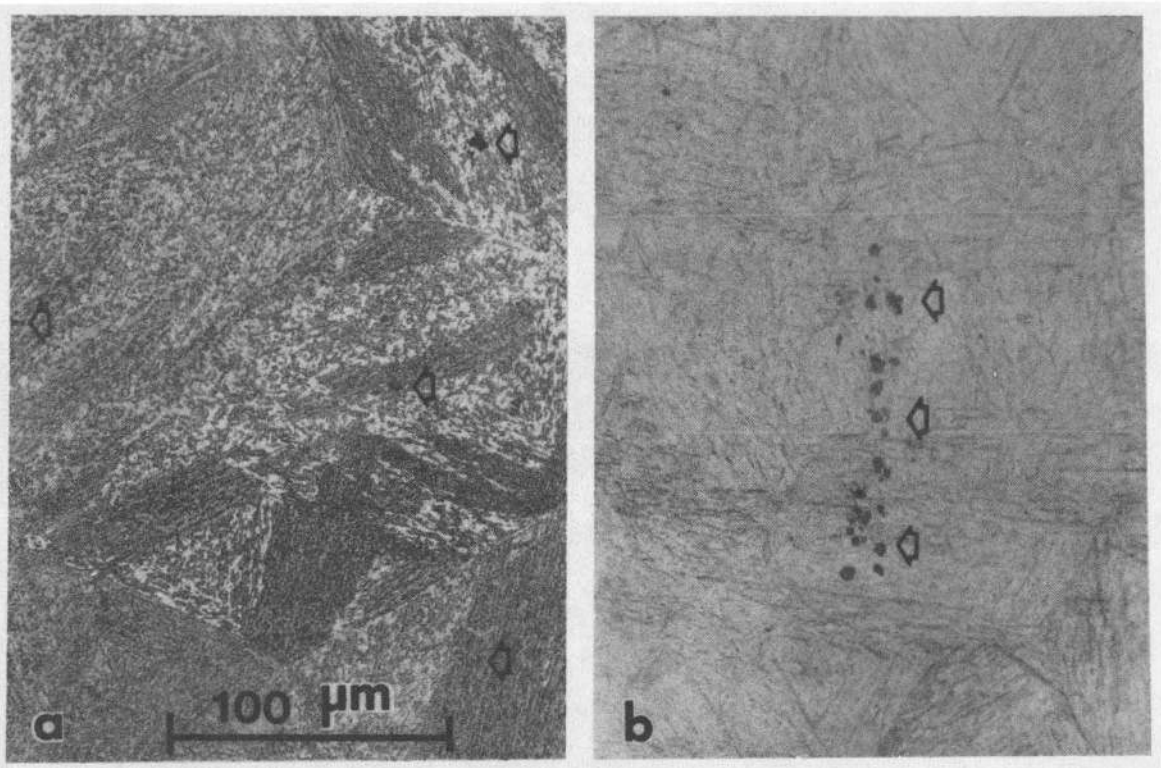

Fig. 3

XBB 800-12615

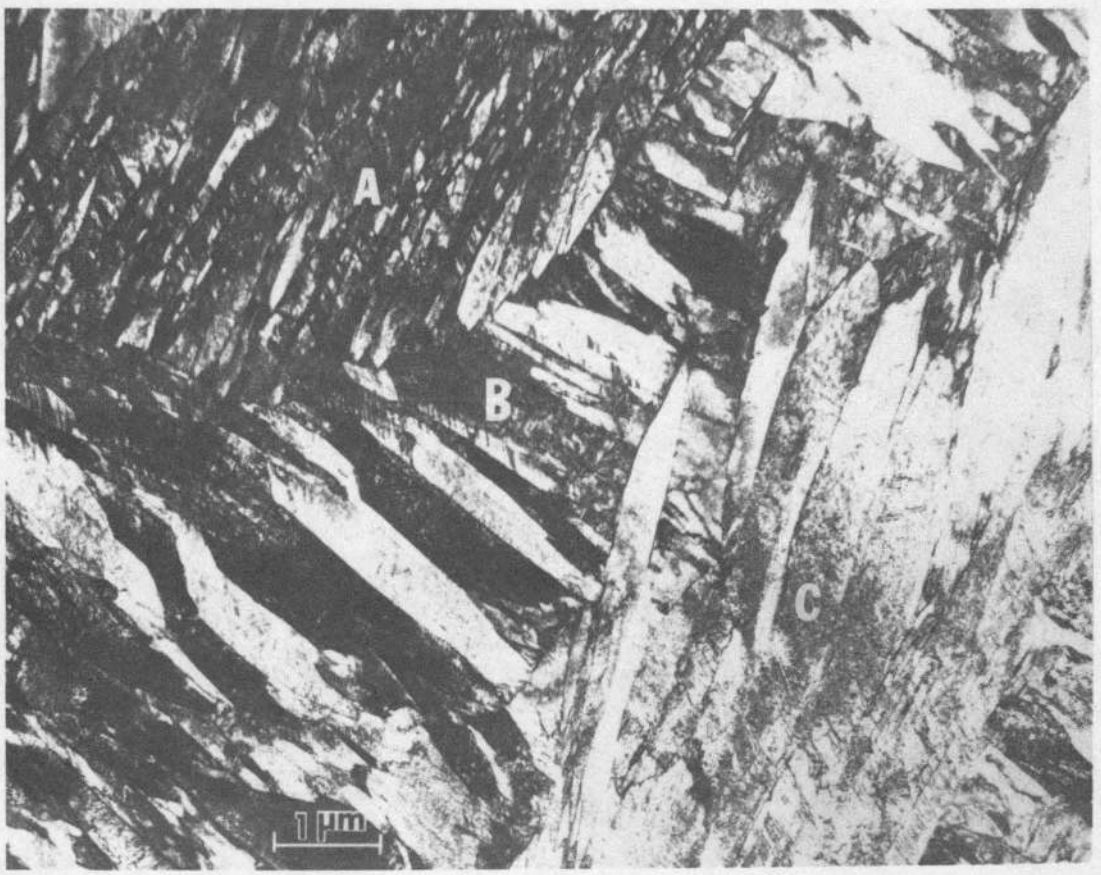

Fig. 4

XBB 800-12616

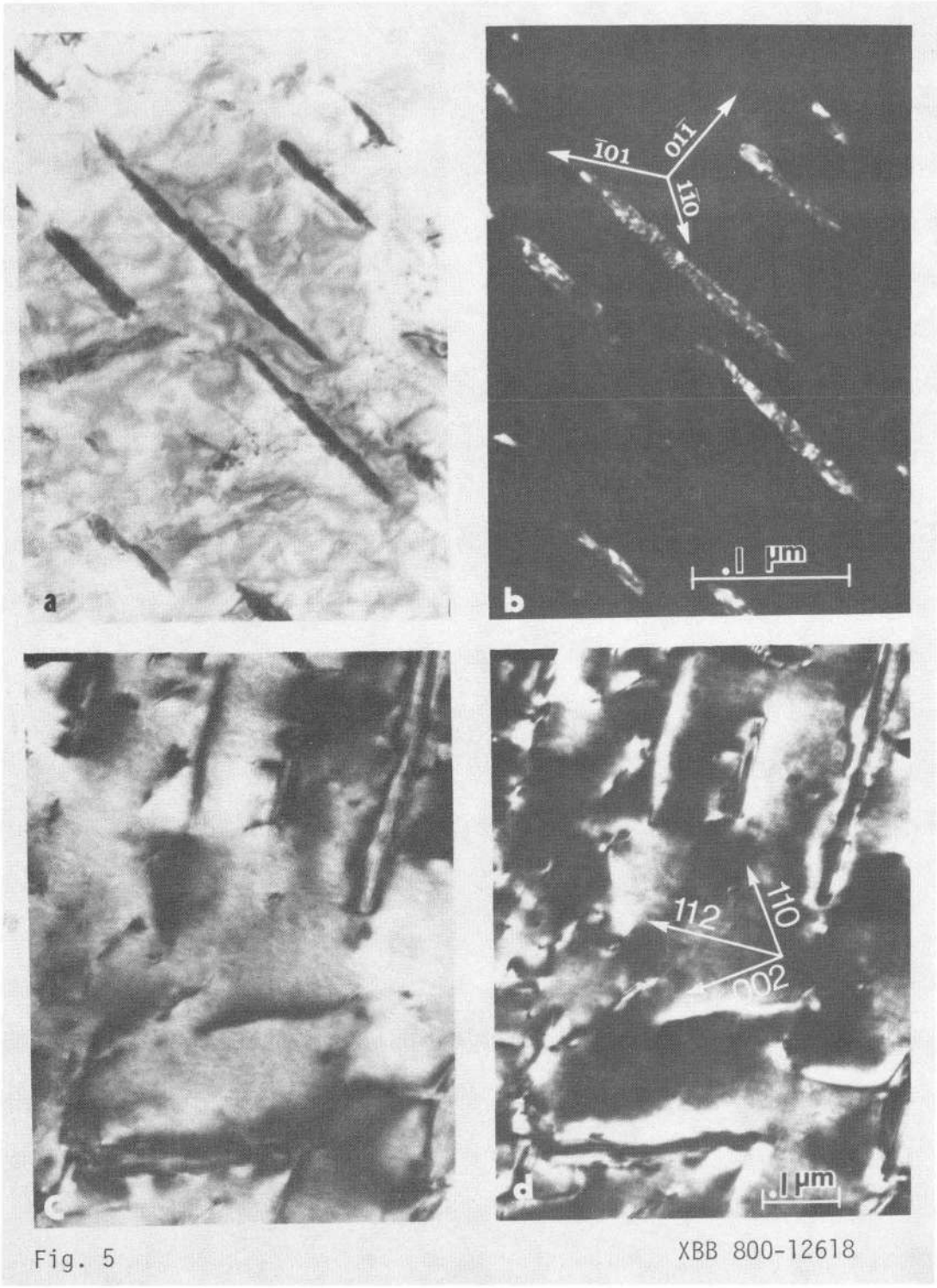

Fig. 5

XBB 800-12618

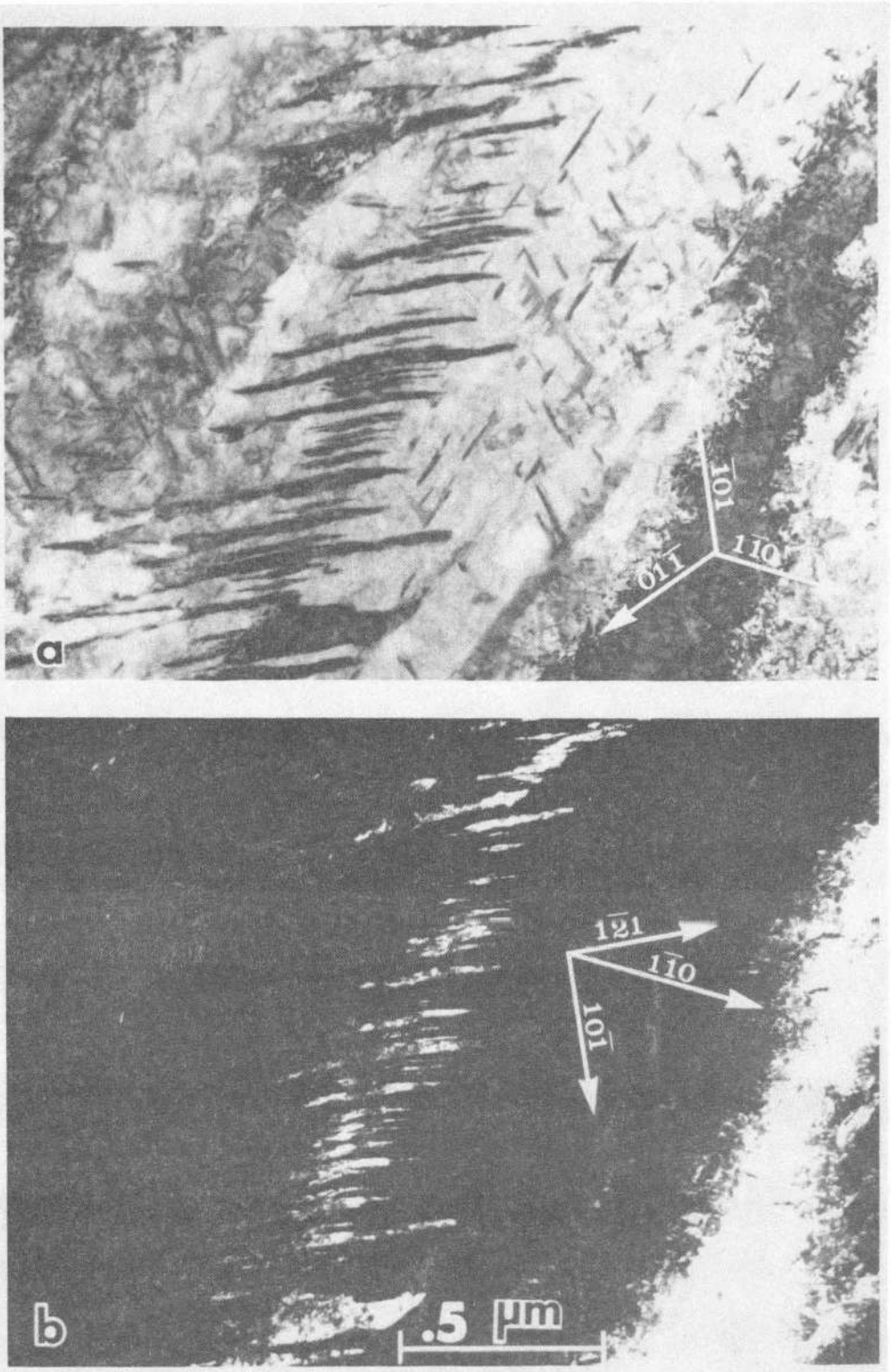

Fig. 6

XBB 794-5823

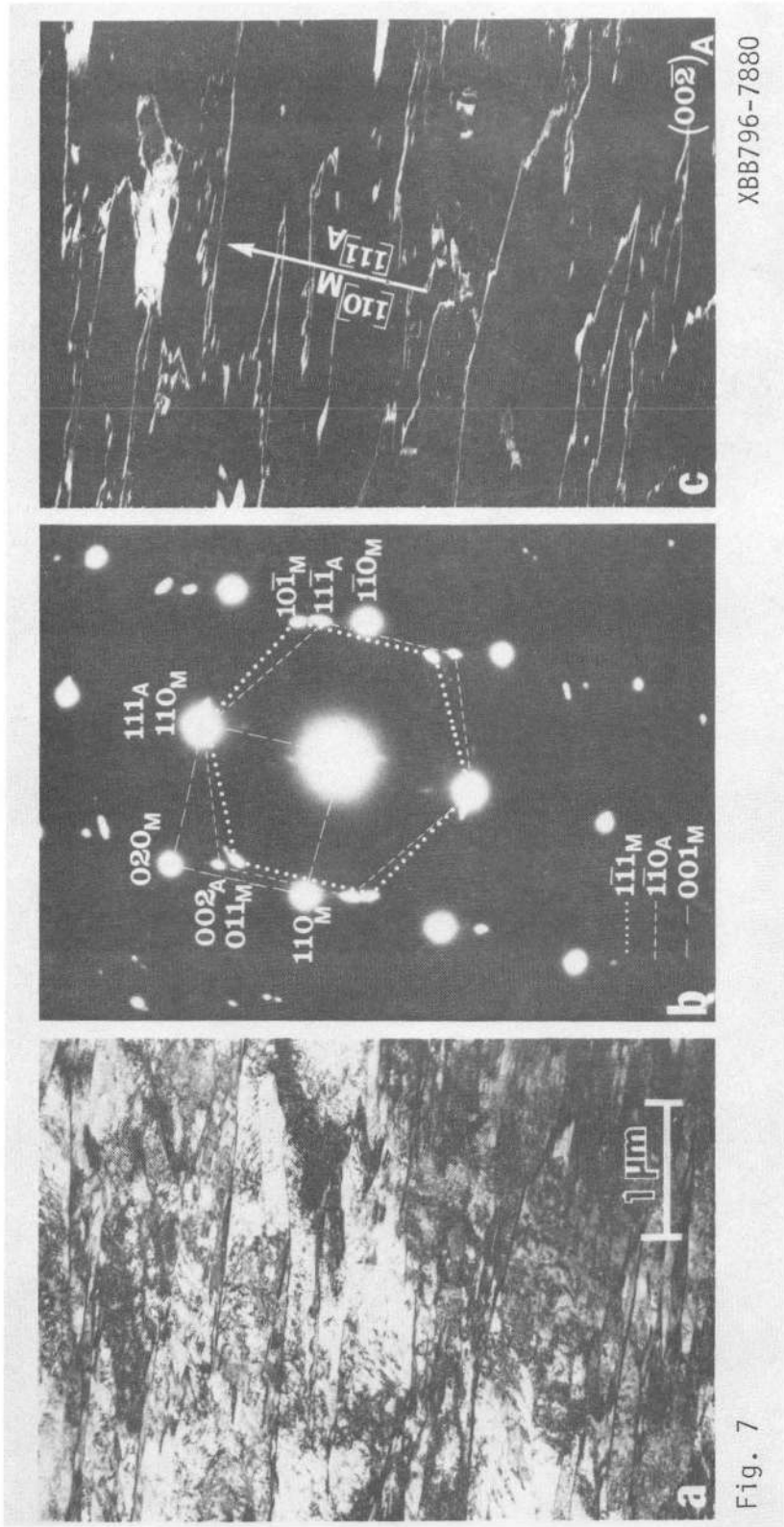

Fig. 7

XBB796-7880

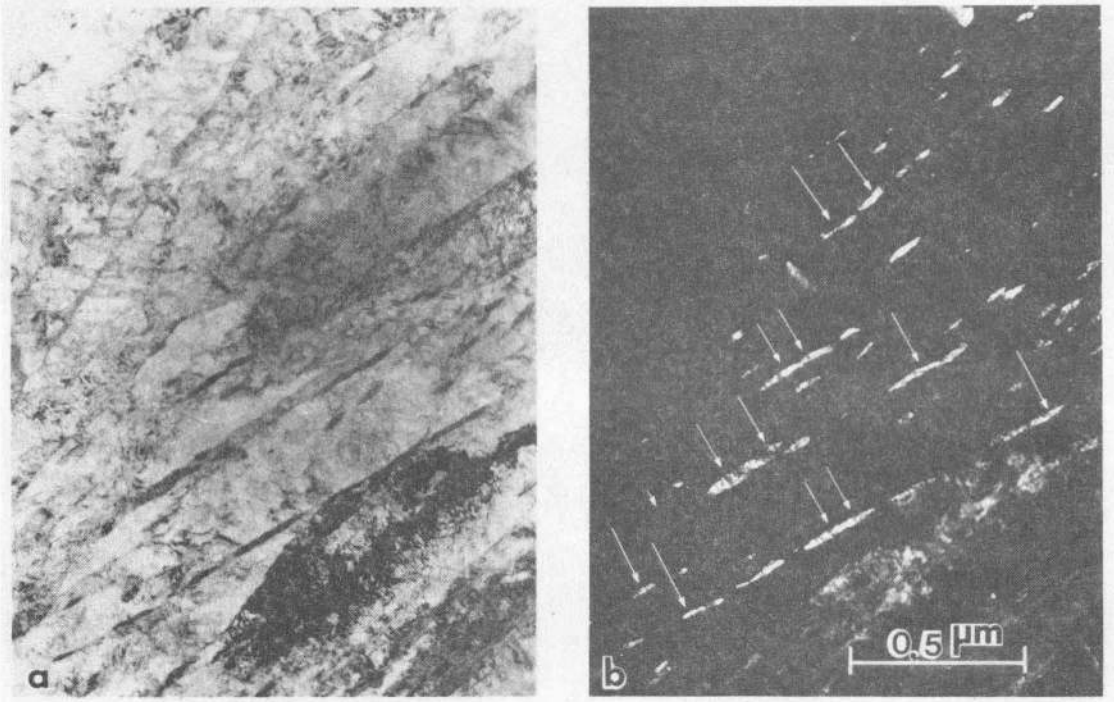

Fig. 8

XBB 794-5669

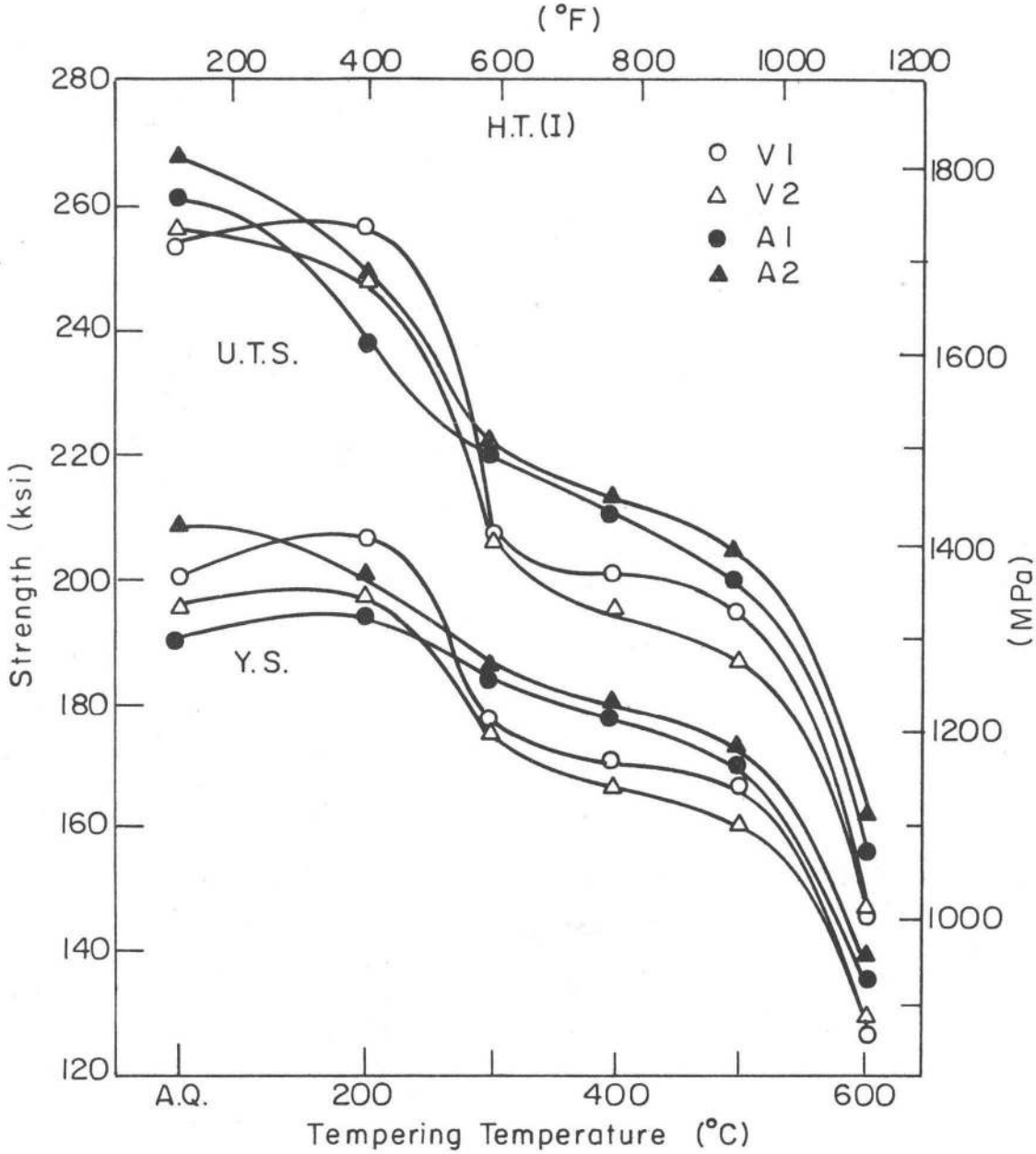

Fig. 9

XBL 8010-6232

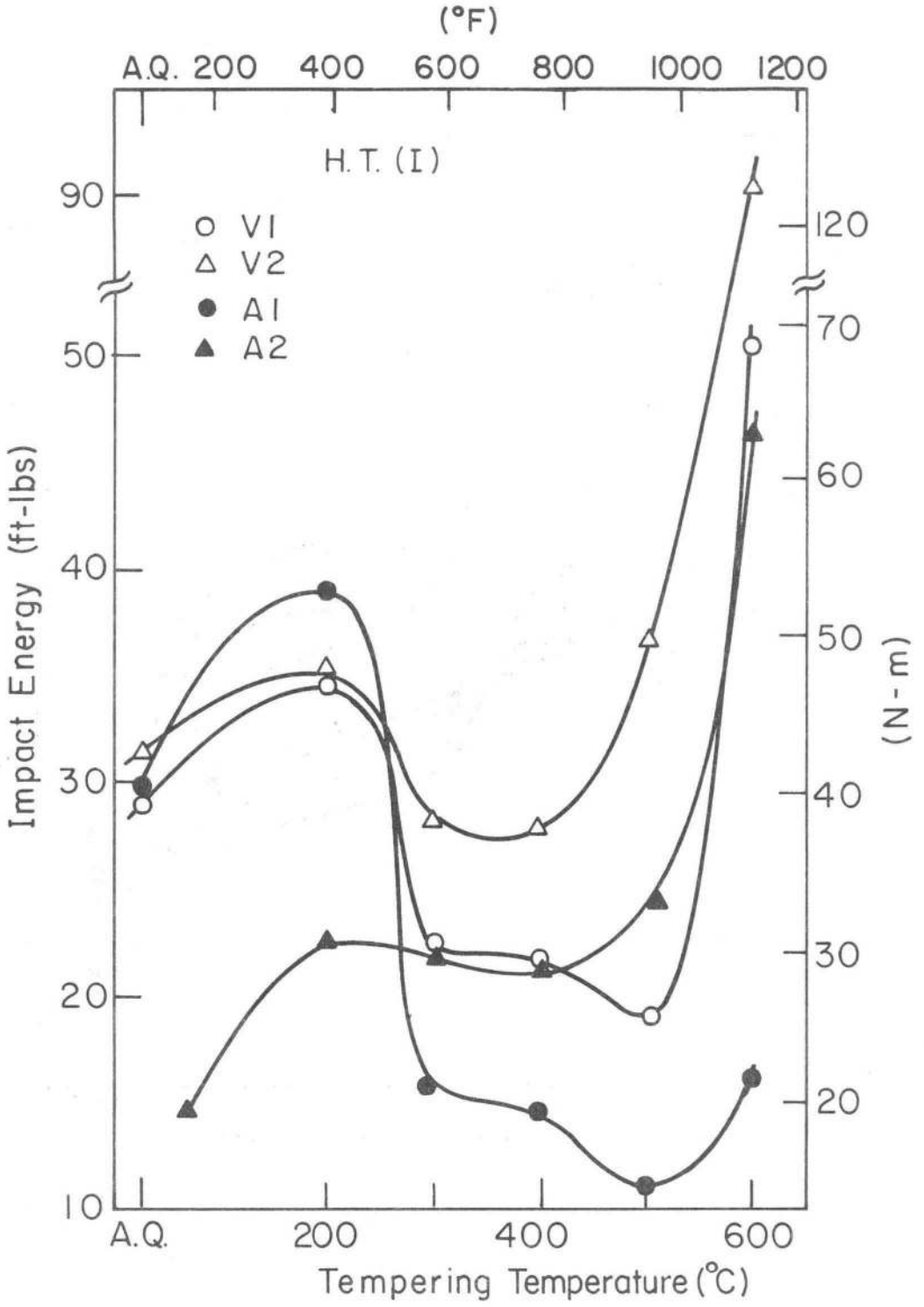

Fig. 10

XBL 8010-6230

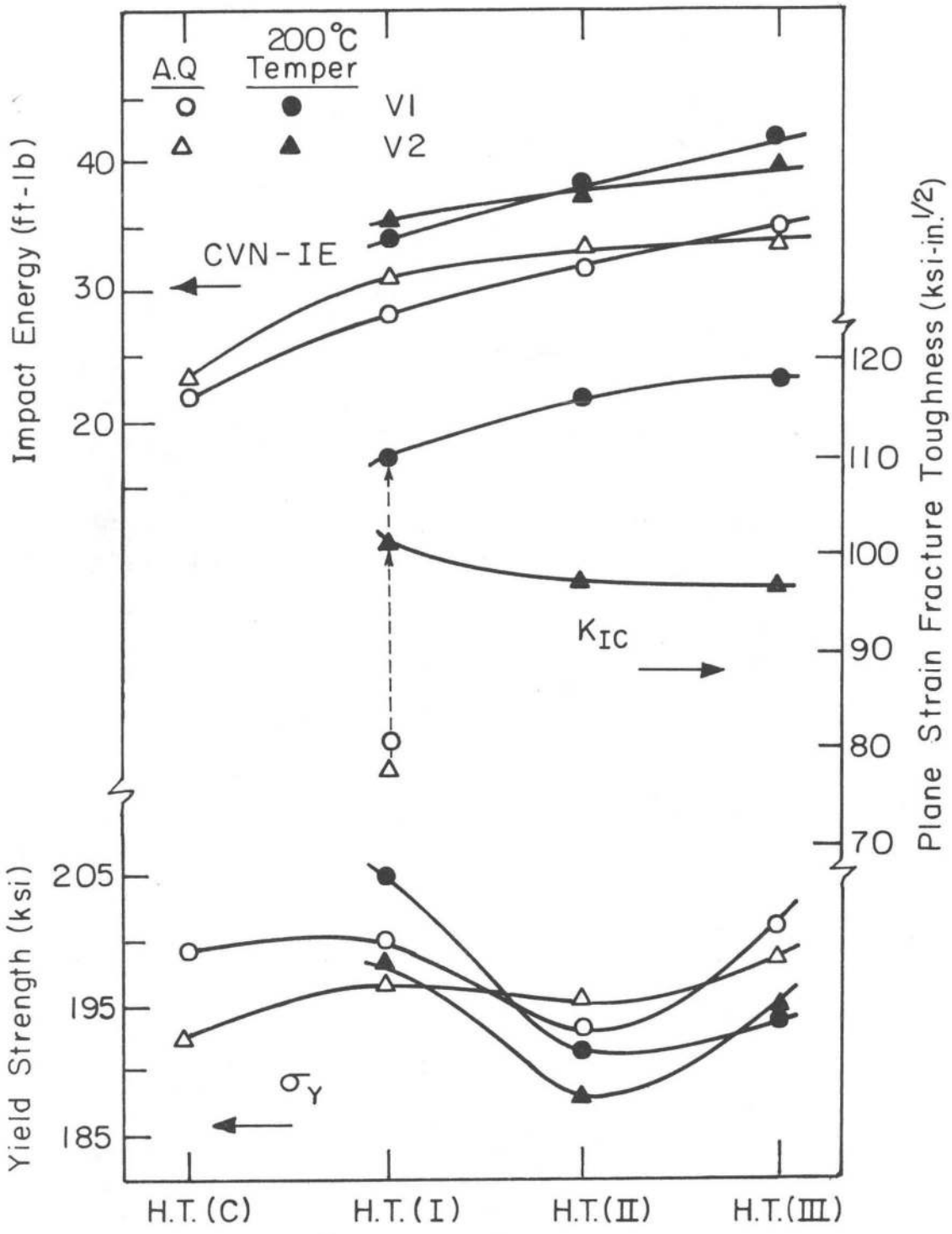

XBL 8010-6233

Fig. 11

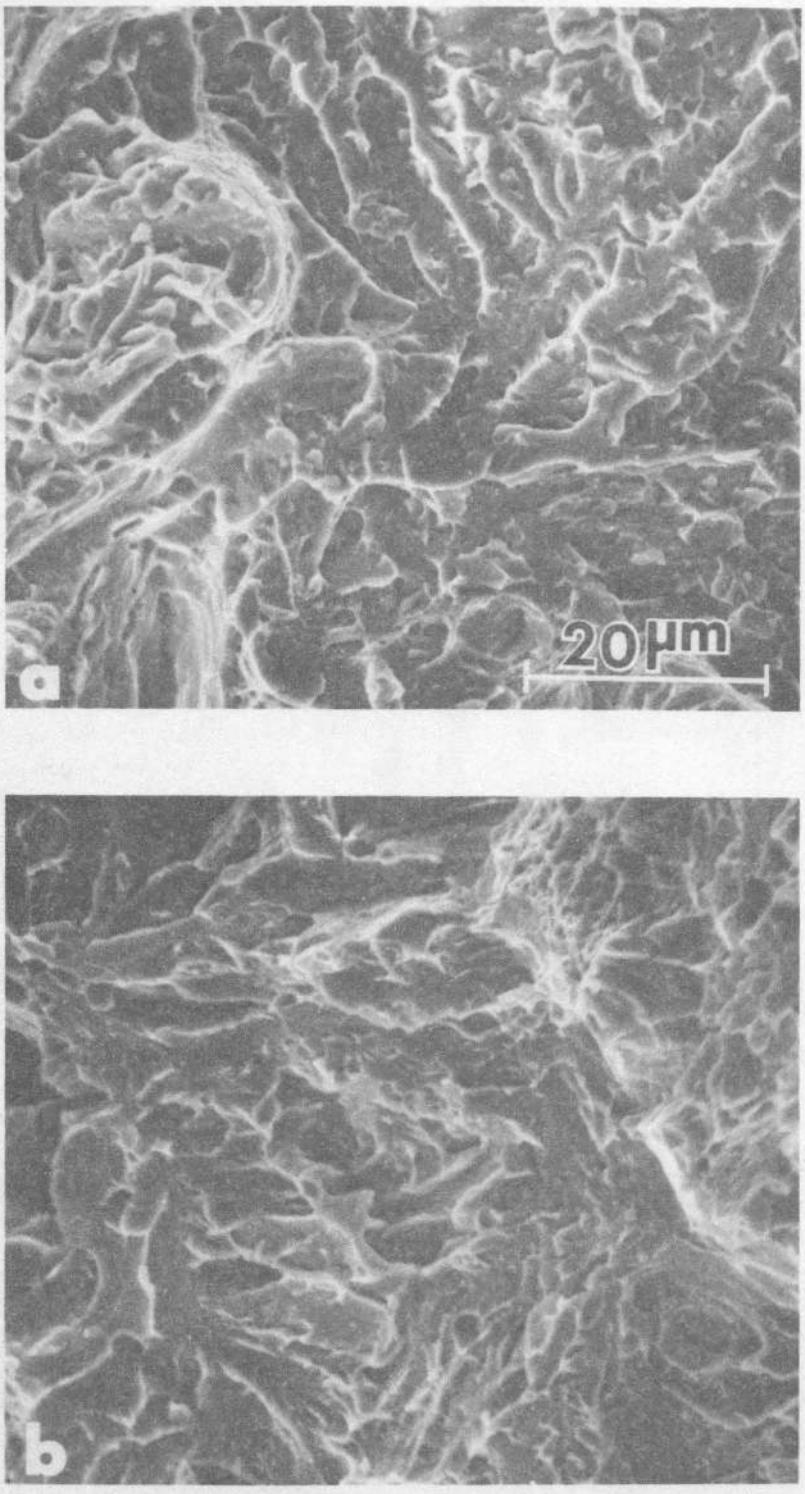

Fig. 12 XBB 794-5470

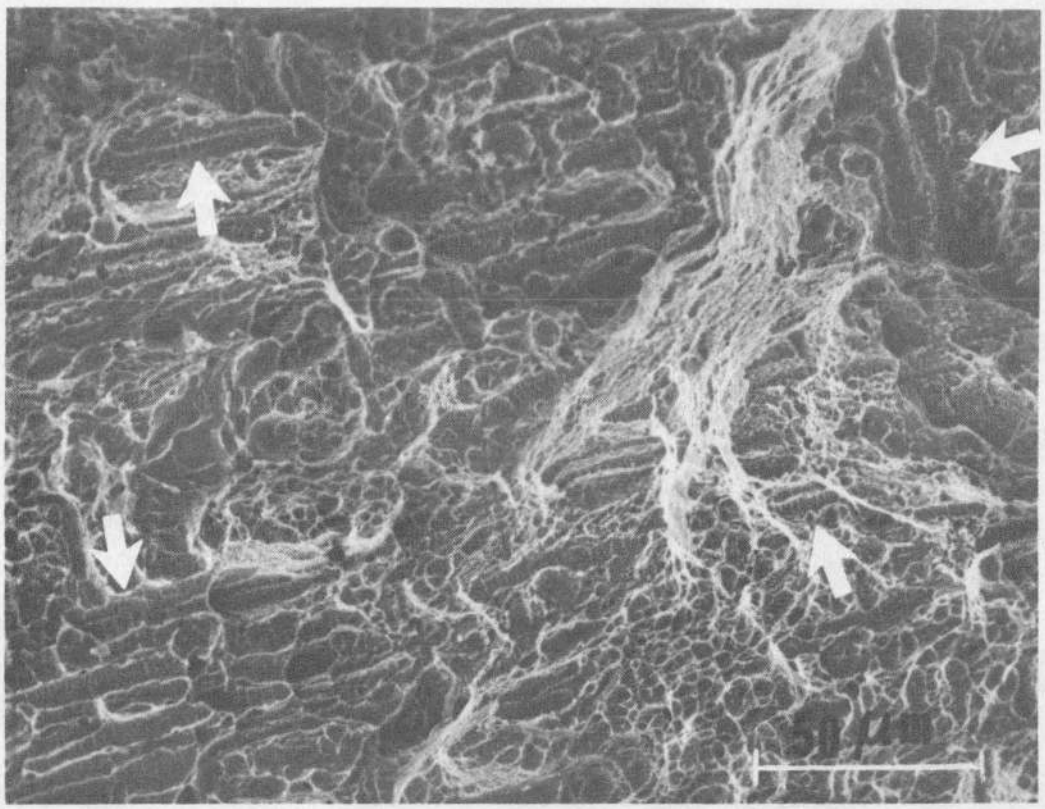

Fig. 13 XBB 780-15409

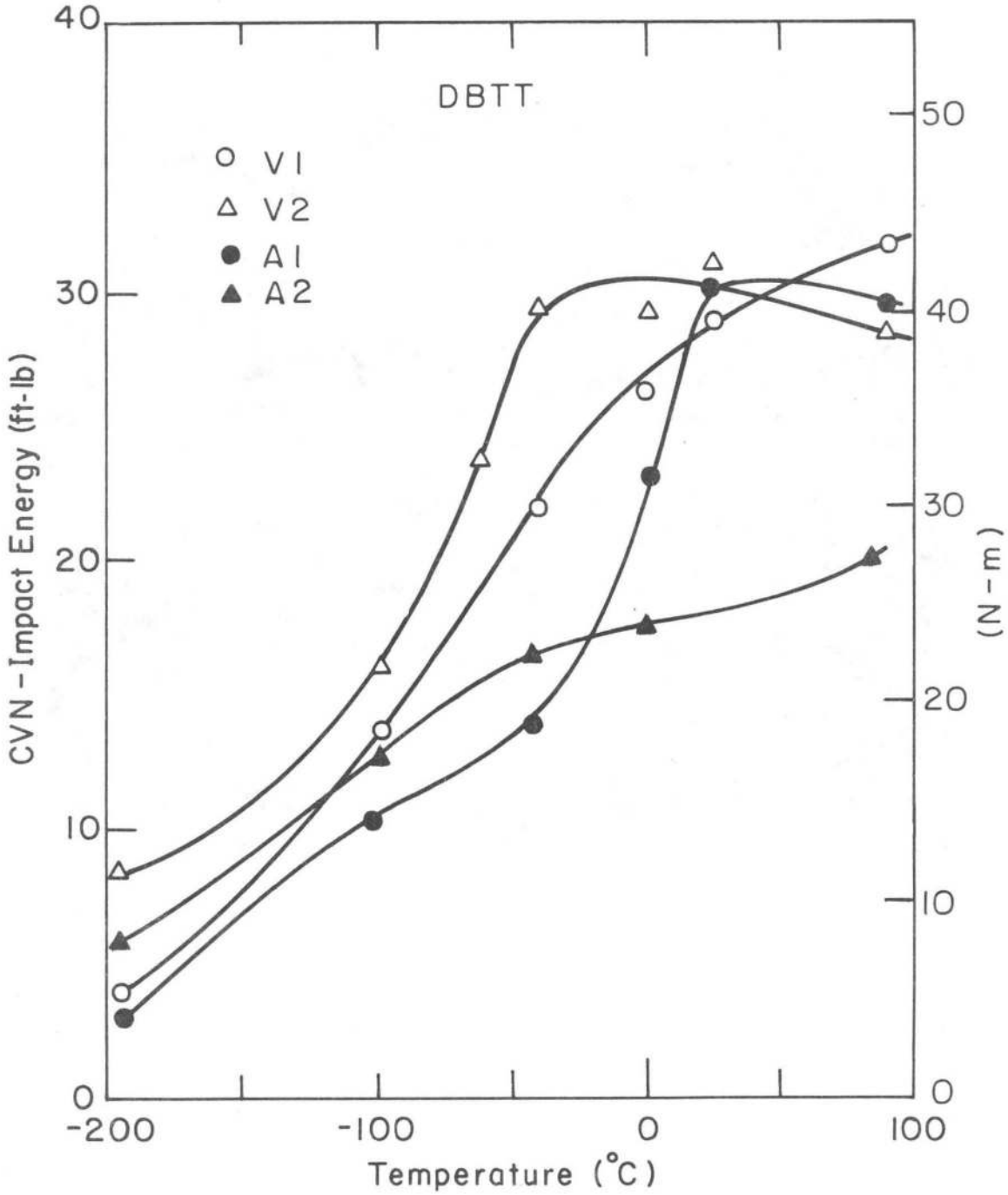

Fig. 14

XBL 8010-6231

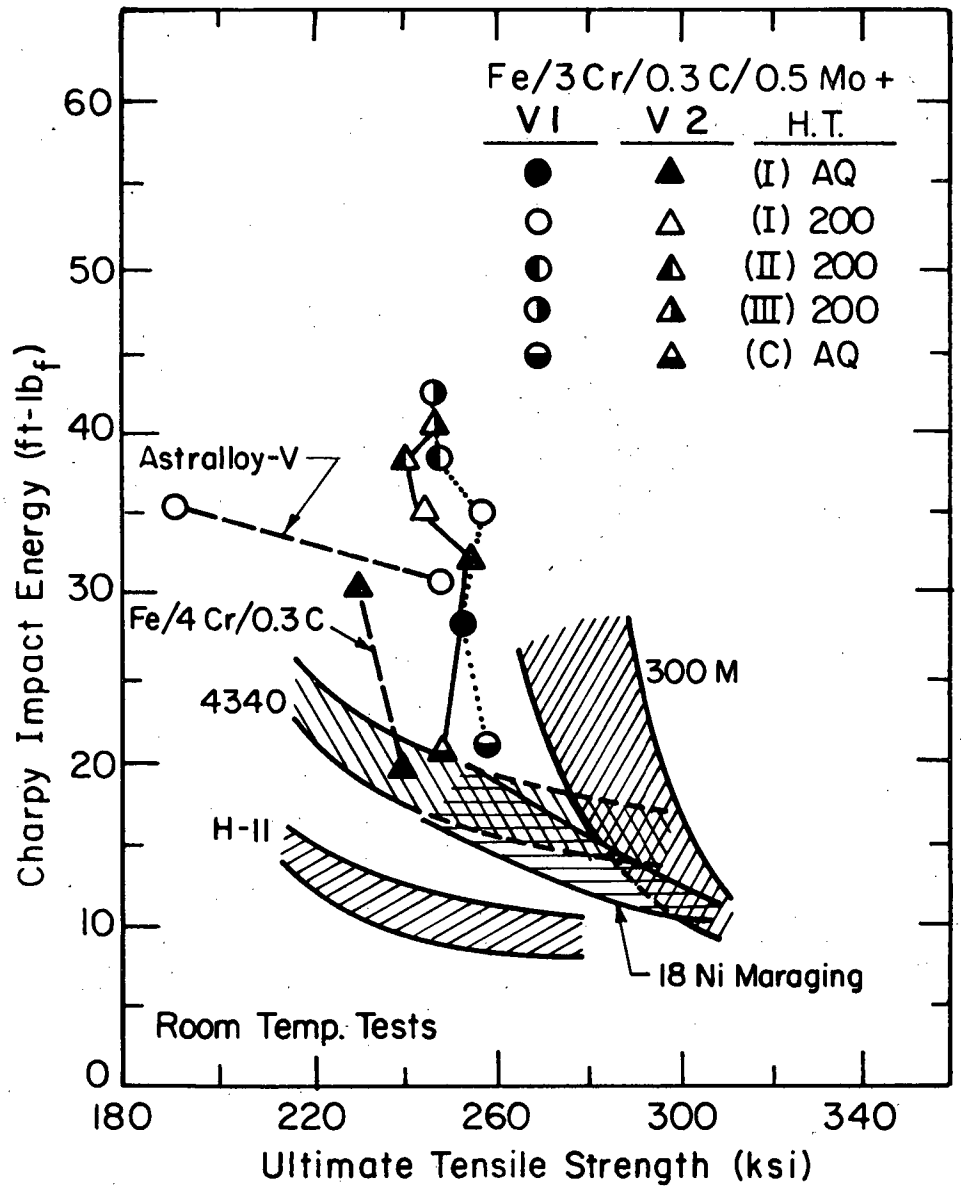

Fig. 15a

XBL 8010-6229

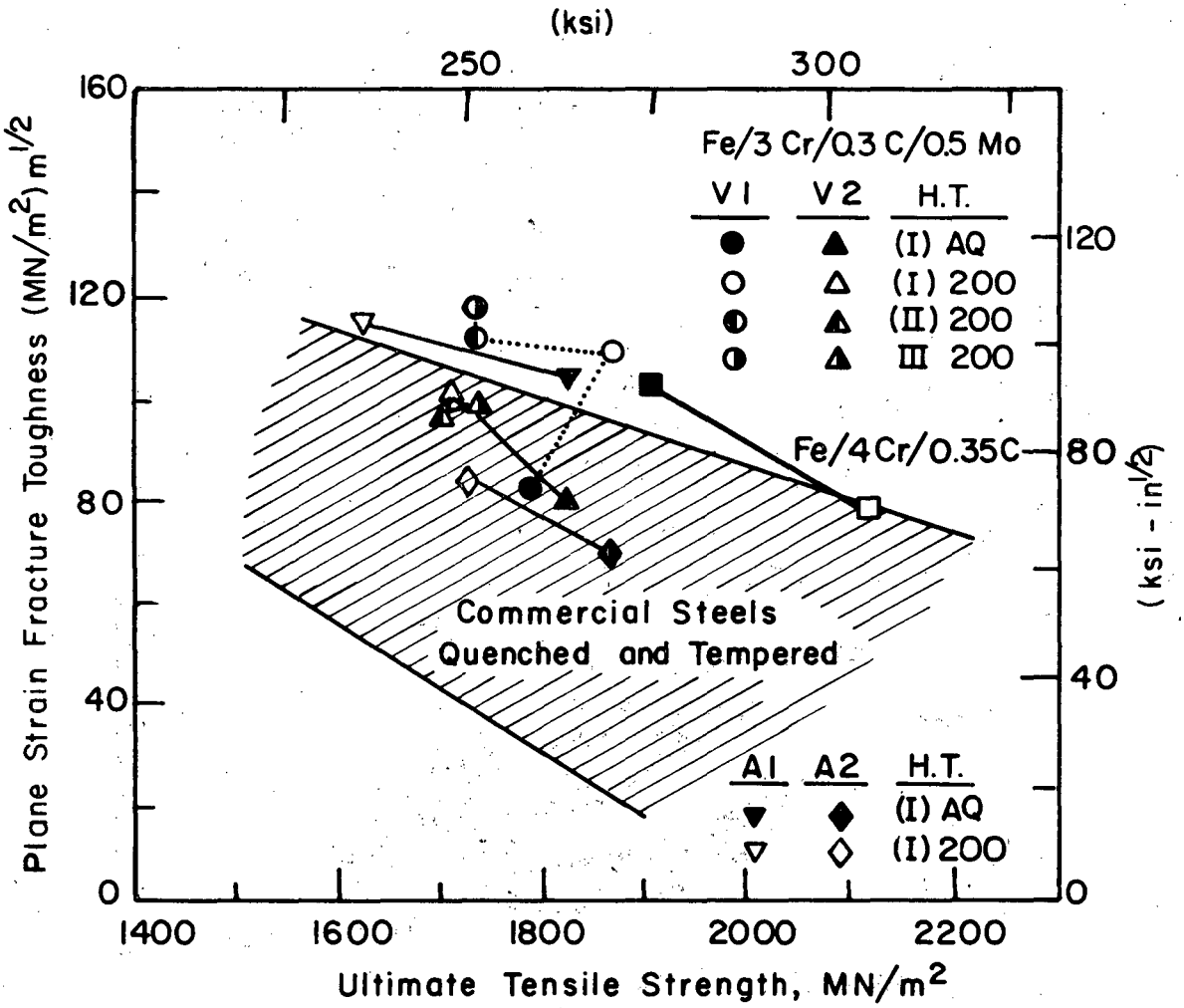
(ksi)
250
300
160
120
80
40
0
Plane Strain Fracture Toughness (MN/m²) m^1/2
Fe/3 Cr/0.3 C/0.5 Mo
V1 V2 H.T.
(I) AQ
(I) 200
(II) 200
III 200
Fe/4Cr/0.35C
120
80
40
0
(ksi - in^1/2)
Commercial Steels
Quenched and Tempered
A1 A2 H.T.
(I) AQ
(I) 200
1400
1600
1800
2000
2200
Ultimate Tensile Strength, MN/m²
XBL 8010-6228

Fig. 15b

This report was done with support from the Department of Energy. Any conclusions or opinions expressed in this report represent solely those of the author(s) and not necessarily those of The Regents of the University of California, the Lawrence Berkeley Laboratory or the Department of Energy.

Reference to a company or product name does not imply approval or recommendation of the product by the University of California or the U.S. Department of Energy to the exclusion of others that may be suitable.

TECHNICAL INFORMATION DEPARTMENT
LAWRENCE BERKELEY LABORATORY
UNIVERSITY OF CALIFORNIA
BERKELEY, CALIFORNIA 94720